Journal of Materials Chemistry C

Accepted Manuscript

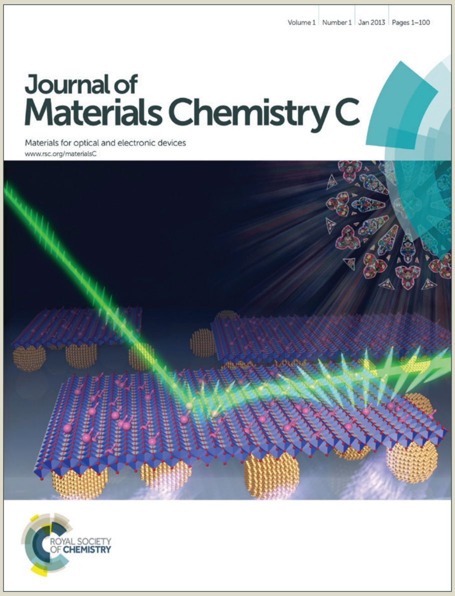

ROYAL SOCIETY OF CHEMISTRY

www.rsc.org/materialsC

Electromagnetic wave absorption of multi–walled carbon nanotubes (outer diameter 8–15 nm)–epoxy composites in R band

Zhou Wang and Guang–Lin Zhao*

Received Xth XXXXXXXXXX 20XX, Accepted Xth XXXXXXXXX 20XX
First published on the web Xth XXXXXXXXXX 200X
DOI: 10.1039/b000000x

Multi–walled carbon nanotubes (MWCNTs)–epoxy composites with MWCNTs (outer diameter between 8–15 nm) loadings from 0.1 to 5 wt.% were fabricated. The morphology, conductivity, dielectric permittivity, and electromagnetic (EM) wave absorption of the MWCNTs–epoxy composites were investigated. The results showed that the EM wave absorption strongly depended on the complex permittivity of the composites. An abrupt enhancement of conductivity by 9 orders of magnitude for the composite sample with 5 wt.% MWCNTs loading is observed, which is associated with a sharp improvement of electromagnetic absorption in R band (26.5–40 GHz) and is characterized by the formation of a conductive network structure consisting of separated MWCNT aggregates and connected MWCNT bundle bridges in the composites. The electrically conductive composite allows the ease of charge transportation between the conductive MWCNT components and contributes to the substantial improvement of electromagnetic absorption of the MWNCTs–epoxy composites.

1 Introduction

Electromagnetic–wave absorbing (EMA) materials are designed to provide electromagnetic absorption, attenuation, and shielding to protect human and electronics from external radiation and find their widely applications as protective materials in modern technologies including satellite communication, TV signal transmission, microelectronic devices, and other applications.[1–6] There is a continuous demand for the development of effective EMA materials in commercial and civilian applications. When exposing to an electromagnetic field, the electrons in the EMA materials can generate an inductive current which can cause the attenuation of electromagnetic wave in the form of heat dissipation.[7]

Traditional EMA materials such as ferrites provide sufficient EMA shielding in many fields. However, ferrites have heavy weight and tend to be corroded. In the last several years, carbon nanotubes (CNTs)–polymer composites have been emerged as one of the prospective EMA materials. The unique 1–D hollow tubular structures of CNTs allow the electrons to transport freely over long length along the z–axial direction and enable them to show good electrical and electromagnetic response. Theoretical analysis also predicts that CNTs possess extreme high tensile moduli and strength as well as high flexibility, which are proved by some experimental data.[8,9] The combination of electrical and mechanical properties of CNTs enables them to be an idea filler and reinforcement agents suitable for the fabrication of EMA composite materials.[10]

In recent years, CNTs–polymer composites are the subject of intensive research. It is known that the dispersion of conductive fillers into polymer and elastomer matrix has great influence on the mechanical and electrical properties of composite materials. Generally, dispersions of filler in polymer matrix evolve with the processing of sonication and/or shear–mixing. A typical sonication process often offers high energy density that is delivered into the solution to separate the aggregates and produce relatively well dispersion. However, the sonication can also induce fracture and scission of CNTs during sonication process, which may deteriorate the ultimate performance of the composites.[11] Moreover, the dispersed and separated CNTs after sonication will reaggregate during following mixing and cast process. The shear–mixing processing is expected to delivery much lower energy density to the mixture. However, it causes relatively mild modification of morphology and physiochemical properties of CNTs after dispersion.

Although a conductive matrix can be formed by uniformly dispersing CNT bundles in the composites, it was recently reported that a composite morphology comprises phase separated regions of aggregates and dangling bridges and can result in more electron transport than an evenly–dispersion CNT network.[12–17] Huang et al. studied the conductivity of multi–walled carbon nanotubes (MWCNTs)–PDMS (poly–dimethylsiloxane) composites by shear–mixing with different stirring time. They found that the increasing mixing time will lead to a dramatic decrease in conductivity, where well–mixed samples became effectively insulating.[12] This counter–

Physics Department, Southern University and A&M College, Baton Rouge, Louisiana, United States. Tel: +1 225 771 4491; E-mail: Guang–Lin_Zhao@subr.edu

intuitive effect was theoretically explained by a recent study which indicates a multi–component CNT dispersion can improve electric percolation than a single phase.[18] However, investigation on the relationship of CNT loadings and morphologies as well as their effects on the conductivity, dielectric properties, and EMA absorption in MWCNTs–epoxy composites is still scarce and remains to be explored, which motivates the major objective of this work.

In this study, MWCNTs–epoxy composites with different MWCNTs (outer diameter (OD) between 8–15 nm) weight loadings were fabricated by a mechanical shear–mixing method. The aim of this work is to investigate how the loading and morphology of MWCNTs in the epoxy matrix will affect the conductivity, dielectric properties, and the EMA performance of the MWCNTs–epoxy composites in R band. A possible EMA mechanism of the composites is discussed, based on the changes of dielectric properties of the composites which are derived from the dispersion of multi–components MWCNTs.

2 Experiment

The MWCNTs were obtained from a commercial company (Cheaptubes, US). The outer diameters of MWCNTs are between 8–15 nm. The length distribution of MWCNTs is in the range of 10–50 μm. The purity of MWCNTs is better than 95 %. The ash content in the MWCNT powder is less than 1.5 wt.%.

MWCNTs–epoxy composites were fabricated via a mechanic shear mixing method. The MWCNT loadings were controlled from 0.1 to 5 wt.%. Firstly, the epoxy resin and MWCNTs were mixed and blended using a hotplate magnetic stirrer at 90 °C for 1 h. The relatively high temperature was used to reduce the viscosity of the mixture. Then a curing agent was added into the mixture and stirred for 10 min at room temperature. After that, the mixture was carefully casted into a hollow square wave guide mold (7.1 mm×3.5 mm×2.0 mm) and transferred to a vacuum oven for pre– and post–curing at 80 and 120 °C, respectively. Both the curing process lasted for 1 h. Thin disc samples with diameter of 120 mm and thickness of 1 mm were also prepared for the measurement of dc conductivity.

The dc conductivity of the composite samples was obtained from the measurement of resistivity of thin disc samples by using a high resistance tester (ZC36, Shenzhen Abeat Technology Co., Ltd, China). Each sample was tested at least three times for better accuracy. The error bar of the measurement data was determined by averaging measured conductivity data points.

Field Emission Scanning Electron Microscopy (FESEM) (Hitachi S–4500 II, Japan) was used to examine the cross–section morphology of the MWCNTs–epoxy composite samples with an acceleration voltage of 5 KV. Prior to each FESEM measurement, the samples were gold coated for good conductivity.

The complex dielectric permittivity $\varepsilon = \varepsilon' - j\varepsilon''$ of the MWCNTs–epoxy composite samples were measured by utilizing Agilent Network Analyzer N5230c (Agilent Company, USA), a wave guide measurement method, and Agilent 85071 materials measurement software for a frequency range from 26.5 to 40.0 GHz.

3 Results and discussions

3.1 FESEM Analysis

Fig. 1 shows the FESEM images of pristine MWCNTs and the cross–section morphologies of MWCNTs–epoxy composite samples. It is observed that individual MWCNTs are entangled with each other and form curved bundles, due to the weak van der Walls interaction between them (Fig. 1(a)).[19]

For the composite samples with 0.1 wt.% MWCNT loading (Fig. 1(b)), isolated MWCNT aggregates are observed. When MWCNT loading increases to 1 wt.%, MWCNT aggregates and scattered MWCNT bundles are also observed which are randomly distributed in the composite matrix (Fig. 1(c)). Further increasing MWCNT loading to 3 and 4 wt.%, the size of MWCNT agglomerations increase as well as the presence of sparse MWCNT bundles (Fig. 1(d) and (e)). However, for the composite sample with 5 wt.% MWCNT loading, continuous MWCNT network are clearly observed, including large MWCNT aggregates and a great amount of individual MWCNT bundles (Fig. 1(f)).

It is clear that MWCNTs–epoxy composites consist of inhomogeneous multi–component networks including MWCNT aggregates and MWCNT bundles. It is also observed that during the slicing process of the composite material, some of the MWCNTs bundles were pulled out from the surface (as shown in the insets of Fig. 1), suggesting the weak (non–chemical bonding) interaction between the MWCNTs and the epoxy host. The relatively weak interaction between MWCNTs with the host matrix may allow MWCNTs to vibrate under the illumination of EM wave, and contribute to the improvement of EMA performance of the composites, which will be further discussed in the next sections.[12]

3.2 DC conductivity analysis

Fig. 2 shows the dc conductivity of MWCNTs–epoxy composites as a function of CNT content. The incorporation of conductive MWCNTs (electrical conductivity >100 S/m) increases the conductivity of the composites. When the MWCNT loadings increases from 0 to 4 wt.%, the conductivity of the composites gradually increases from $\sim 2.2 \times 10^{-15}$

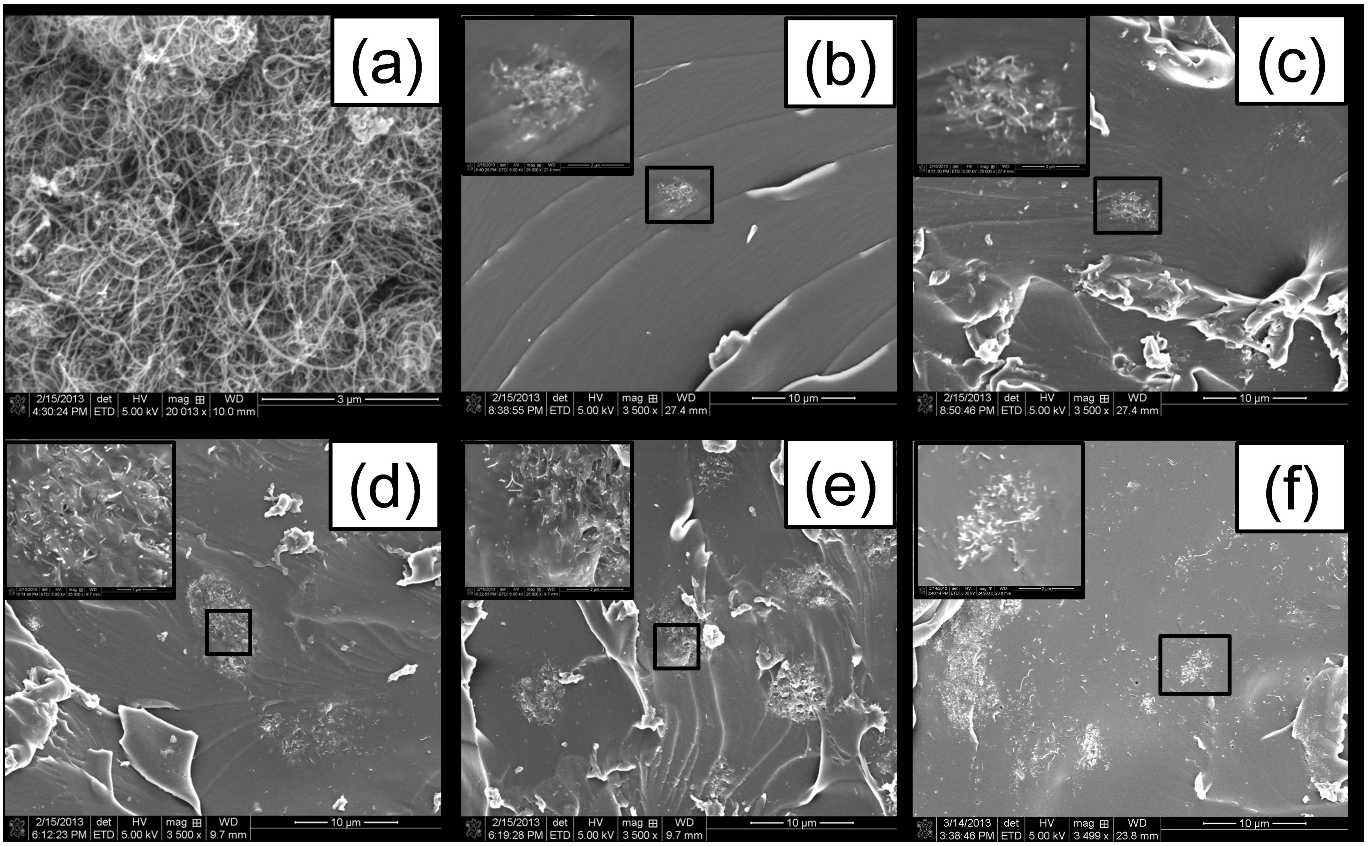

Fig. 1 FESEM images of (a) pristine MWCNTs; and the cross–sections of MWCNTs–epoxy composites at different MWCNT loadings, (b) 0.1 wt.%, (c) 1 wt.%, (d) 3 wt.%, (e) 4 wt.%, and (f) 5 wt.%. The insets on the upper–left of (b)–(f) show the regions in the black box with higher magnifications.

to $\sim 4.4 \times 10^{-12}$ S/m, that is mainly due to the intrinsic conductivity of MWCNTs. Further increasing the MWCNTs loading to 5 wt.%, the conductivity of the composites substantially increases to $\sim 2.0 \times 10^{-3}$ S/m. The abrupt increase of conductivity of the composites by almost 9 orders of magnitude clearly indicates that the electric conductivity of the MWCNTs–epoxy composite sample is not merely due to the intrinsic conductivity of the MWCNTs.

The properties can be understood by the percolation theory for charge transport, which also involves the effective electron tunneling or hopping.[20,21] The percolation threshold in the composites occurs when the MWCNTs loading is around 5 wt.%. It indicates a transition from an insulating state to a more conductive state in the composite, due to a formation of continuous conductive network throughout the insulating polymer matrix.

In light of the morphology analysis as discussed earlier, it can be concluded that the conductive structures in the composite is comprised with MWCNTs aggregates and MWCNTs bundles which bridge together by electron tunneling through

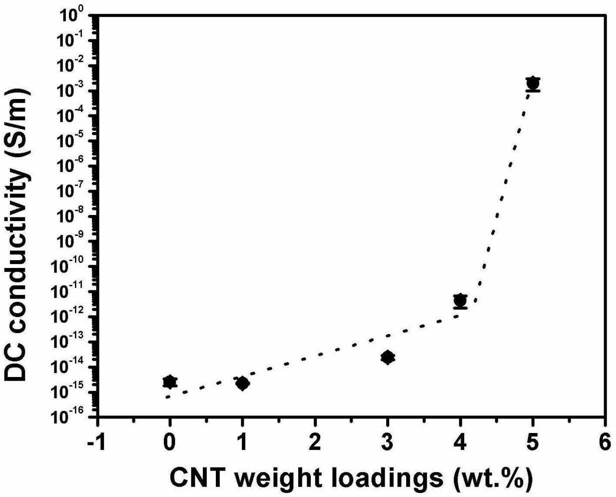

Fig. 2 DC conductivity of MWCNTs–epoxy composites with different MWCNT loadings. The dash line is a guide for the data.

the polymer. The high conductivity of the composites with 5 wt.% MWCNT loading indicates a synergetic percolation due to the interplay between the various conductive components in the MWCNTs–epoxy composites, which is consistent with previous reports on a highly conducting system due to the conductive chain of aggregates spanning the whole sample.[12,18] The percolation thresholds in MWCNTs–polymer composites may depend on the types of MWCNTs, the matrix material, and the processing methods.

3.3 Complex Dielectric Permittivity

Relative complex permittivity ε and permeability μ are the fundamental physical quantities related to the electromagnetic wave absorption of the MWCNTs–epoxy composites. The relative complex permeability μ of the MWCNTs–epoxy composites are very low and do not show much feature, due to the weak magnetic characteristics of both epoxy resin and MWCNTs. The electromagnetic wave absorption of the MWCNT–epoxy composite samples is mainly attributed to their dielectric properties.

The MWCNTs consist of a blend of metallic and semi–conducting nanotubes. The dielectric response of the MWCNTs–epoxy composites is mostly related to the electric properties of the metallic CNTs, whilst the semi–conducting CNTs can be viewed as effectively increasing of the permittivity of the MWNCTs–epoxy composites.[22,23] When EMA materials are exposed to an external electromagnetic field, the radiation will induce two types of electric currents in the materials. One is the conduction current due to the presence of free electrons in the materials and the other one is the displacement current due to bound charges.[24] The conduction current contributes to the imaginary part of permittivity and causes dielectric loss, which represents the ability of a material to dissipate the energy from an external electromagnetic field and convert it to heat. The displacement current mainly contributes to the real part of permittivity which is due to polarization effects involving unpaired point defects and polarized interfaces.[25,26] The real part of the complex permittivity ε' represents the ability of a material to store the energy from an external electromagnetic field.

Fig. 3(a) shows the real part ε' of the relative complex permittivity of MWCNTs–epoxy composite samples. The increase of real part of permittivity is related to the dielectric relaxation and space–charge effects. The ε' slightly increases from ~ 2.4 for pure epoxy to ~ 2.6 for the composites with 0.1 wt.% MWCNTs loading, indicating that the addition of 0.1 wt.% loading amount of MWCNTs to the composites does not have too much effects on the dielectric property of the MWCNTs–epoxy composites. Further increasing the MWCNTs loadings from 0.5 to 4 wt.%, ε' gradually raises from ~ 3.2 to ~ 6.4 and do not show much frequency–dependence in the measured frequency range. When the MWCNT loading is 5 wt.% in the MWCNTs–epoxy composite, ε' reaches about 10.0 and also show frequency–dependence in the measured range. The ε' is 10.8 at 26.5 GHz and lineally decreases to 9.0 at 40 GHz.

Fig. 3(b) shows the imaginary part of relative complex permittivity ε'' of the MWCNTs–epoxy composites. The ε'' of the pure epoxy sample and the MWCNTs–epoxy composites with 0.1 wt.% MWCNTs loading are very low and are less than 0.1. When the MWCNT loadings in the composites increase from 0.5 wt.% to 4 wt.%, ε'' gradually increases from ~ 0.3 to ~ 1.5. Especially, when the MWCNT loading in the composite increases to 5 wt.%, the ε'' substantially rises to about 4.5 and show some frequency–dependence. The increase of imaginary part of permittivity is related to the improvement of electric conductivity in the composites that is consistent with the conductivity analysis as discussed in the previous section.

The loss tangent related to the permittivity is defined as: $tan\delta = \varepsilon''/\varepsilon'$, which is a measure of the energy loss due to the dielectric response of the material.[27] Fig. 3(c) shows that the dielectric loss tangent of MWNCTs–epoxy composites increases as the MWNCT loadings increase in the composites. A substantial enhancement of the loss tangent is observed from ~ 0.2 to ~ 0.5 when the MWNCT loadings increase from 4 to 5 wt.%, which resembles the tendency of conductivity and imaginary part of permittivity ε'' of the MWCNTs–epoxy composites.

3.4 Electromagnetic Wave Absorption Properties of the MWCNTs–Epoxy Composite in R–Band

The EM wave incident on a material surface can be reflected, absorbed, and transmitted. MWCNTs–epoxy composites can attenuate the EM wave and absorb the EM wave energy. The total energy of the EM wave (taken as unity 1) can be described as the summation of reflectance (R), Absorbance (A), and transmittance (T). The absorbance (A) denotes the fraction of incident energy power that is absorbed throughout the sample.[28–32] In this study, the EM absorption of the MWCNTs–epoxy composites is evaluated by measuring the scattering parameters (S–parameters): the reflection coefficient (S11 or S22) and transmission coefficient (S12 or S21) which were directly obtained from the Agilent vector analyzer. According to the classic transmission line theory, we can obtain,[31]

$$R = |S11|^2 = |S22|^2 \tag{1}$$

$$T = |S21|^2 = |S12|^2 \tag{2}$$

$$A = 1 - R - T \tag{3}$$

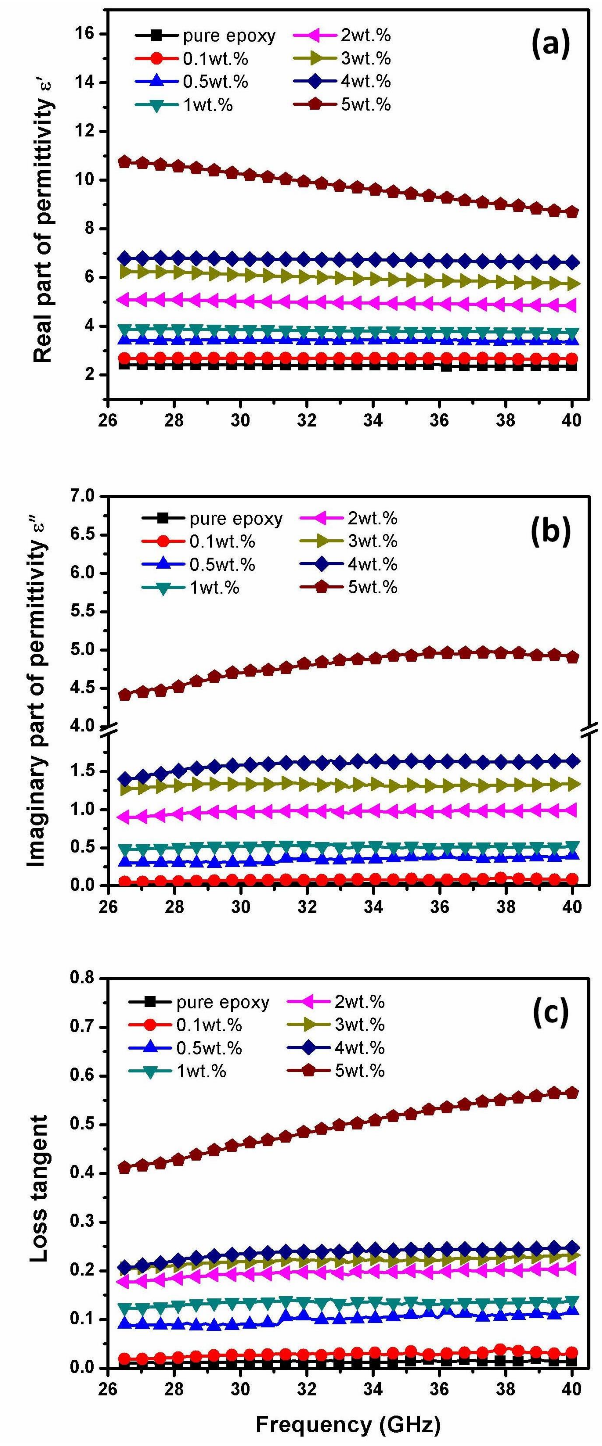

Fig. 3 Real part, imaginary part and loss tangent of permittivity of pure epoxy and MWCNTs–epoxy composites with different MWNCT loadings (in wt.%) in R band.

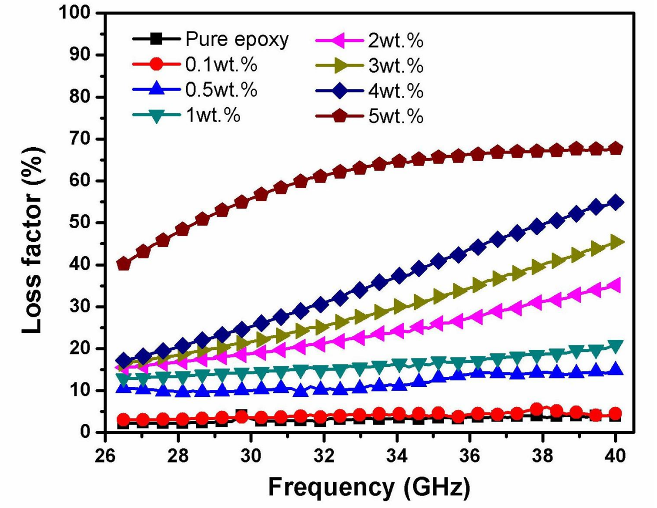

Fig. 4 Loss factor of pure epoxy and MWCNTs–epoxy composites with different MWCNT loadings.

Herein, the EM absorbance A can be calculated from the measured Sparameters and is a measure of the EM wave absorption efficiency of the composite material.

Fig. 4 shows the absorbance of the MWCNTsepoxy composites with different MWCNT loadings in wt.%. When the MWCNT loadings increase to from 0.1 to 0.5 wt.%, the absorbance of the MWCNTs–epoxy composites raises from ∼ 3.0 % to ∼ 10.0 % in the measured frequency range. Further increasing the MWCNT loadings up to 4 wt.%, the absorbance gradually increases and also show frequency dependences. For example, the absorbance of the composite with 4 wt.% MWCNT loading is 17 % at 26.5 GHz and rises to 53 % at 40 GHz. Most distinctly, the MWCNTs–epoxy composite sample with 5 wt.% MWCNT loading show an astonishing enhancement in its EM wave absorbance and more pronounced frequency dependence (Fig. 4). The absorbance of this sample is 40 % at 26.5 GHz and increases to 67 % at 40 GHz.

Previous report attributed the defects in CNTs as polarization center and improve the complex permittivity of the composites, which leaded to the contribution of the enhancement of EM absorption.[1] However, the CNTs in our composite samples are not expected to introduce a large amount of defects by considering that a relatively mild mechanical mixing was used in the fabrication process. Mdarhri et al. proposed that the interfaces and boundaries between MWCNTs and the epoxy matrix can contribute to the enhancement of EM absorption due to the interaction of external radiation and the charge multipoles at the interfaces.[33] However, the interfacial interaction between the CNTs and epoxy in the composites is relatively weak as discussed early in the FESEM section due to the non–chemical bonding between MWCNTs and epoxy. So the defects in CNTs and interfaces in the composites are not the main contributions to the EM absorption of the composite samples in this study.

When exposed to an external electromagnetic field, the electrons in the EM absorbing materials will generate an inductive current. This will cause the attenuation of external electromagnetic wave and convert it to heat. For CNTs, the electrons are restricted in the 1–D tubular graphitic structure and can move freely along the *z*–axial direction, which provides good conductivity for MWCNTs. The individual MWCNTs and MWCNT aggregates in the epoxy composites can attenuate and dissipate the radiation via the interaction between the interior electrons and external electromagnetic field, which contributes the EM absorption of MWCNTs–epoxy composites.

Herein, for the composite samples with MWCNTs loading increasing from 0.1 to 4 wt.%, the main contribution to the EM absorption is due to the intrinsic conductive properties of MWCNT bundles and aggregates. The free electrons in CNTs will interact with EM waves and contribute to the EM absorption of the composites. Interestingly, a substantial increase of complex permittivity, loss tangent and loss factor are observed for the composites with 5 wt.% MWCNT loading, indicating an abrupt improvement of EM absorption of the composites. The MWCNTs–epoxy composites are characterized by the formation of an electrically conductive network in the composites. The main contribution to the enhancement of electromagnetic wave absorption is suggested to be as follows: the external electromagnetic radiation will induce induction current in the conductive network due to the conductive charge transportation between different MWCNT components in the composites which will in turn strongly interact with the electromagnetic wave, contributing to the improvement of EM absorption performance in the MWCNTs–epoxy composites due to dielectric loss. Our results demonstrate that a multi–component structure comprised with separated MWCNT aggregates and connected MWCNTs bundle bridges contributes to the substantial enhancement of EM absorption of the MWCNTs–epoxy composites.

4 Conclusions

In this work, MWNCTs-epoxy composites with MWCNT loadings from 0.1–5 wt.% were fabricated by mechanically shearing mixing. The results showed that, for the composite samples with MWCNT loadings up to 4 wt.%, the main contribution of EM absorption for the composite samples is due to the intrinsic conductivity of MWCNTs. When the MWCNTs loading is 5 wt.%, a substantial enhancement of conductivity, complex permittivity, and EM absorption of the composites was observed. We demonstrated that the formation of a multi–component conductive network structure in MWCNTs–epoxy composites consisting of MWCNTs aggregates and continuous MWCNT bundle bridges contributes to the substantial improvement of the EM wave absorption of the composites. The results show that the composite with 5 wt.% MWCNTs has good EM attenuation performance and can be used as EMA materials in R band for shielding electronics and wireless communication devices, and as light-weight protective and EMA coatings.

5 Acknowledgment

The work is funded in part by the Air Force Office of Scientific Research (Award No FA9550-09-1-0367 and FA9550-11-1-0330) and NSF LASIGMA Project (Award No. EPS-1003897, NSF92010-15-RII-SUBR).

References

1 P. C. P. Watts, W. K. Hsu, A. Barnes and B. Chambers, *Adv. Mater.*, 2003, **15**, 600–603.

2 R. K. Srivastava, T. N. Narayanan, A. P. R. Mary, M. R. Anantharaman, A. Srivastava, R. Vajtai and P. M. Ajayan, *Appl. Phys. Lett.*, 2011, **99**, 113116–3.

3 X. Sun, J. He, G. Li, J. Tang, T. Wang, Y. Guo and H. Xue, *J. Mater. Chem. C*, 2013, **1**, 765–777.

4 F. Qin and C. Brosseau, *J. Appl. Phys.*, 2012, **111**, 061301–24.

5 Z. Wang, G. Wei and G.-L. Zhao, *Appl. Phys. Lett.*, 2013, **103**, 183109.

6 M.-M. Lu, W.-Q. Cao, H.-L. Shi, X.-Y. Fang, J. Yang, Z.-L. Hou, H.-B. Jin, W.-Z. Wang, J. Yuan and M.-S. Cao, *J. Mater. Chem. A*, 2014, **2**, 10540–10547.

7 Z. Wang and G.-L. Zhao, *Open J. Comp. Mater.*, 2013, **03**, 17–23.

8 J. N. Coleman, U. Khan, W. J. Blau and Y. K. Gunko, *Carbon*, 2006, **44**, 1624–1652.

9 A. Pullen, G. L. Zhao, D. Bagayoko and L. Yang, *Phys. Rev. B*, 2005, **71**, 205410.

10 Z. Spitalsky, D. Tasis, K. Papagelis and C. Galiotis, *Prog. Polym. Sci.*, 2010, **35**, 357–401.

11 C. J. Kerr, Y. Y. Huang, J. E. Marshall and E. M. Terentjev, *J. Appl. Phys.*, 2011, **109**, 094109–6.

12 Y. Y. Huang and E. M. Terentjev, *Adv. Funct. Mater.*, 2010, **20**, 4062–4068.

13 N. A. Chowdhury, J. Robertson, A. M. Al-Jumaily and M. V. Ramos, *J. Mater. Chem. C*, 2013, **1**, 8041–8045.

14 C. Yang, C. P. Wong and M. M. F. Yuen, *J. Mater. Chem. C*, 2013, **1**, 4052–4069.

15 S. S. Rahatekar, M. S. P. Shaffer and J. A. Elliott, *Compos. Sci. Technol.*, 2010, **70**, 356–362.

16 G.-W. Huang, H.-M. Xiao and S.-Y. Fu, *J. Mater. Chem. C*, 2014, **2**, 2758–2764.

17 W.-L. Song, M.-S. Cao, M.-M. Lu, J. Liu, J. Yuan and L.-Z. Fan, *J. Mater. Chem. C*, 2013, **1**, 1846–1854.

18 A. V. Kyrylyuk, M. C. Hermant, T. Schilling, B. Klumperman, C. E. Koning and P. Van Der Schoot, *Nat. Nanotechnol.*, 2011, **6**, 364–369.

19 P.-C. Ma, N. A. Siddiqui, G. Marom and J.-K. Kim, *Composites Part A*, 2010, **41**, 1345–1367.

20 W. Bauhofer and J. Z. Kovacs, *Compos. Sci. Technol.*, 2009, **69**, 1486 – 1498.

21 F. Du, R. C. Scogna, W. Zhou, S. Brand, J. E. Fischer and K. I. Winey, *Macromolecules*, 2004, **37**, 9048–9055.

22 C. A. Grimes, C. Mungle, D. Kouzoudis, S. Fang and P. C. Eklund, *Chem. Phys. Lett.*, 2000, **319**, 460–464.
23 Z. Wang, J. Luo and G.-L. Zhao, *AIP Adv.*, 2014, **4**, 017139.
24 T. N. Narayanan, V. Sunny, M. M. Shaijumon, P. M. Ajayan and M. R. Anantharaman, *Electrochem. Solid-State Lett.*, 2009, **12**, K21–K24.
25 P. A. Miles, W. B. Westphal and A. Von Hippel, *Rev. Mod. Phys.*, 1957, **29**, 279–307.
26 C. G. Koops, *Phys. Rev.*, 1951, **83**, 121–124.
27 A. R. Von Hippel, *Dielectrics and waves*, Boston, Artech House, 1995.
28 J. Capwell, T. Weller, D. Markell and G. Dunleavy, L, *Automation and real-time verification of passive component S-parameter measurements using loss factor calculations*, 2004.
29 L. Chen, C. Ong, C. Neo, V. Varadan and V. Varadan, *Microwave Electronics: Measurement and Materials Characterization*, Wiley, 2004.
30 D. Pozar, *Microwave Engineering*, Wiley John & Sons, 2005.
31 D. Micheli, C. Apollo, R. Pastore and M. Marchetti, *Compos. Sci. Technol.*, 2010, **70**, 400–409.
32 J. M. Thomassin, D. Vuluga, M. Alexandre, C. Jerome, I. Molenberg, I. Huynen and C. Detrembleur, *Polymer*, 2012, **53**, 169–174.
33 A. Mdarhri, F. Carmona, C. Brosseau and P. Delhaes, *J. Appl. Phys.*, 2008, **103**, 054303–9.